ELSEVIER

Journal of Chromatography A, 696 (1995) 321–332

JOURNAL OF CHROMATOGRAPHY A

Application of capillary zone electrophoresis with an isotachophoretic initial state to determine anionic impurities on as-polished silicon wafer surfaces

J. Boden[a], K. Bächmann[a,*], L. Kotz[b], L. Fabry[b], S. Pahlke[b]

[a]*Fachbereich Chemie der Technischen Hochschule Darmstadt, D-64289 Darmstadt, Germany*

[b]*Wacker-Chemitronic GmbH, D-84489 Burghausen, Germany*

First received 17 August 1994; revised manuscript received 1 December 1994; accepted 14 December 1994

Abstract

Mobile inorganic anions such as chloride, sulfate and nitrate were determined up to an analyte-to-matrix-ratio (ATMR) of $1:10^4$ using capillary zone electrophoresis. On adjusting the mobility and the concentration of the co-ion of the electrolyte to an isotachophoretic initial state, the detection limit of the analytes was improved by a factor of 2 by increasing the plate numbers through the isotachophoretic state. The ATMR could be increased to $1:6 \cdot 10^4$. These optimized conditions were applied to the determination of anionogenic impurities on experimental silicon wafer surfaces ($d = 150$ mm) after dissolution of the native oxide of silicon in isothermally distilled hydrofluoric acid vapour down to the range of 10^9 anions/cm^2. The mobile organic anion oxalate was identified on silicon wafer surfaces for the first time.

1. Introduction

Metal impurities have a detrimental impact both on the fabrication yield and on the reliability of integrated circuit devices [1]. After decades of scientific investigations, device makers have gained a detailed knowledge of metallic contamination and have developed adequate analytical tools [2,3] and preventive techniques against yield losses due to metallic contamination. However, less is known about the effects of anions [4–6], owing to the lack of sufficient trace analytical methods. Recently, the advancement of capillary zone electrophoresis (CZE) has facilitated its applications to anion trace determinations in the semiconductor industry [7,8].

The determination of small anions in the presence of a matrix ion is a demanding task, because peak broadening of the analyte peaks takes place and preconcentration by electrokinetic injection or sample stacking is not applicable. A possibility for preconcentrating analyte ions in the presence of an inorganic matrix ion is to use a combination of isotachophoresis (ITP) and CZE using a coupling of two capillaries [9–14] or employing ITP and CZE on-line in the same capillary [13–17].

Theoretically, by adjusting the electrolyte composition and the sample amount to realize ITP conditions at the beginning of the CZE run,

* Corresponding author.

0021-9673/95/$09.50 © 1995 Elsevier Science B.V. All rights reserved
SSDI 0021-9673(94)01227-X

a stacking process of the analytes occurs [18] and the matrix issue can be resolved. Thus, the matrix anion must act as either the leading or the terminating species of the CZE separation. At the end of ITP, the analytes with mobilities between those of the matrix ion and the electrolyte co-ion will have been preconcentrated by the ITP. If the analyte mobilities do not lie within that limited range, peak broadening must be expected. Reaching a uniform field strength along the capillary by electromigrative dispersion of the matrix ion, ITP is not longer sustainable. Comparing this method with the conventional ITP technique, we can emphasize a remarkable feature: the leading or terminating electrolyte arises from the matrix ion of the sample and that zone must be formed by a moving boundary mechanism first.

In this paper, we report on applications of CZE to the determination of traces of anions on as-polished silicon wafer surfaces. The method is a combination of microdissolution enrichment, based on the reaction of hydrofluoric acid vapour with the native oxide of silicon [19–21], and CZE with an ITP initial state.

2. Experimental

2.1. CZE system

We used a laboratory-made CZE system. The separations were carried out with conventional untreated fused-silica capillaries (50 and 75 μm I.D.) from CS-Chromatographie Service (Langerwehe, Germany). The capillary was suited with direct insertion for a type ABI 785A programmable absorbance detector (Applied Biosystems, Weiterstadt, Germany) of variable wavelength capability. The outlets were placed in two vials each containing 10 ml of electrolyte. The high voltage from a 30 kV power supply (F.u.G. Electronic, Rosenheim, Germany) was applied with Pt–Ir electrodes dipping into the electrolyte. The positive electrode was placed in the outlet vessel. Data were processed by an A/D board from ERC (Alteglofsheim, Germany) using APEX chromatography software (Autochrom, Milford, MA, USA). The absorbance units of the detector were transformed by the A/D board into μV, hence the output of the data was in the voltage mode.

2.2. Chemicals

All solutions, electrolytes and standards were prepared with ultra-pure water from a Milli-Q system (Millipore, Eschborn, Germany). For microdissolution, hydrofluoric acid (50%, S-ULSI Puranal) from Riedel-de Häen (Seelze, Germany) was applied. All other reagents were of analytical-reagent grade from Merck (Darmstadt, Germany).

Tetradecyltrimethylammonium hydroxide (TTAOH) was prepared from tetradecyltrimethylammonium bromide (TTAB), as described previously [22], using IRA-904 Amberlite anion-exchange resin (Serva, Heidelberg, Germany).

2.3. Sample preparation

All samples were prepared under clean-bench conditions (Class 1 by Federal Standard 209 C, VDI-2083) in poly(vinylidene fluoride) (PVDF) chambers. The dissolution enrichment technique applied has been described [19–21]. The hydrophobic HF-etched surface of as-polished and cleaned wafers (d = 150 mm) was scanned with a droplet of ultra-pure water (100 μl) to collect the dissolved contaminants. The water droplet was transferred with an Eppendorf (Hamburg, Germany) pipette into a freshly cleaned 250-μl Eppendorf vial. Recovery rates were investigated for bromide and sulfate after preparation runs.

3. Results and discussion

3.1. CZE determination of small inorganic anions in hydrofluoric acid matrix

In order to achieve a symmetrical peak shape in CZE with indirect UV detection, an electrolyte with a high molar absorptivity should be

Table 1
Mobilities of some analyte ions and electrolyte co-ions [24]

Parameter	Electrolyte			
	Chromate	Molybdate	Phthalate	Salicylate
$\mu[(cm^2/V \cdot s) \cdot 10^{-4}]$	8.1	7.4	5.5	3.7

	Analyte					
	Bromide	Chloride	Sulfate	Nitrate	Chlorate	Fluoride
$\mu_{lit}[(cm^2/V \cdot s) \cdot 10^{-4}]$	8.1	7.9	8.3	7.4	6.7	5.7
μ_{eff}[a]$[(cm^2/V \cdot s) \cdot 10^{-4}]$	8.0	7.7	7.6	7.4	6.5	5.3

[a] The effective mobilities μ_{eff} were calculated from an electropherogram without a matrix ion, using molybdate as co-ion (for conditions, see Fig. 1).

applied and the mobility of its co-ion must closely match the mobilities of the analyte ions [23]. For analytes such as chloride, sulfate and nitrate, molybdate was found to have an appropriate mobility (Table 1, Fig. 1). Because of the low wavelength of the absorbance maximum of molybdate (211 nm), nitrate was detected directly owing to its higher absorbance at this wavelength. For all other ions the indirect detection mode obtained.

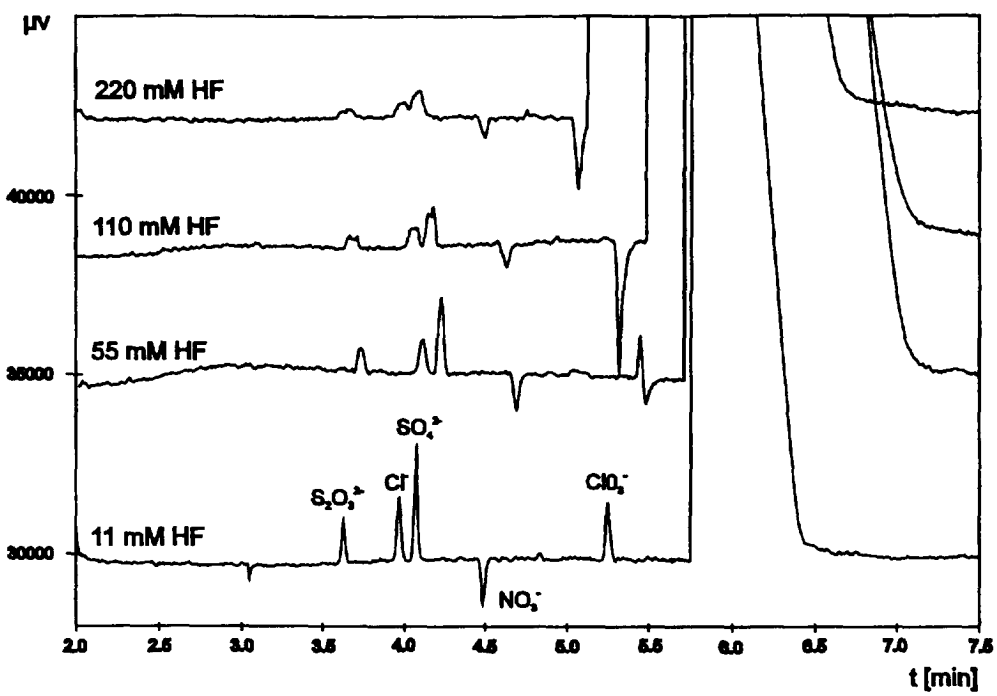

Fig. 1. Influence of HF on the peak heights using molybdate as electrolyte. Electrolyte, 5 m*M* sodium molybdate (pH 6.7); analytes, each 20 μM; capillary, fused silica, 60 cm to the detector, 76 cm total length, 75 μm I.D.; detection, for nitrate direct UV, for all other anions indirect UV at 211 nm; injection, hydrostatic (10 cm, 30 s); EOF, in opposite direction to the anions, $v_{EOF} = 2.7$ cm/min.

The effect of the hydrofluoric acid matrix can be characterized by the peak heights because characterization by plate number or peak area is valid only for Gaussian peaks. Obviously, the peak heights of chloride and sulfate decreased with increasing hydrofluoric acid concentration. Under the described CZE conditions, the analytes of interest can be determined up to an analyte-to-matrix ratio (ATMR) of $1:10^4$.

We investigated the effects of both the capillary I.D. and the electrolyte concentration in order to optimize the CZE conditions. Initially, we compared the separation with a capillary of 75 μm I.D. with that of a capillary of 50 μm I.D. (Fig. 2). As expected, the smaller cross-section of the latter capillary facilitated a better resolution. This is due, on the one hand, to the fact that the resolution is improved with decreasing $(dE)^2$, where d is the diameter and E the field strength, by reduced thermal zone deformation [25]. On the other hand, it is due to the decrease in sample volume (hydrostatic injection, 10 cm, 30 s) because the smaller sample volume prevented overloading of the capillary. A further analysis with a longer injection time in order to achieve a comparable injected amount using the 50 μm I.D. capillary led to the same result (not shown). Therefore, the limitation of the thermal diffusion is the main reason for the better resolution. The electroosmotic flow (EOF) is similar in both capillaries, which leads to comparable migration of the analytes in both capillaries. However, the selected I.D. must be a subtle compromise between electrophoretic resolution and detectability.

Increasing the electrolyte concentration provides additional chemical system capacity. Fig. 3 shows the influence of the electrolyte concentration on the peak heights using a 50 μm I.D. capillary. As expected, additional electrolyte

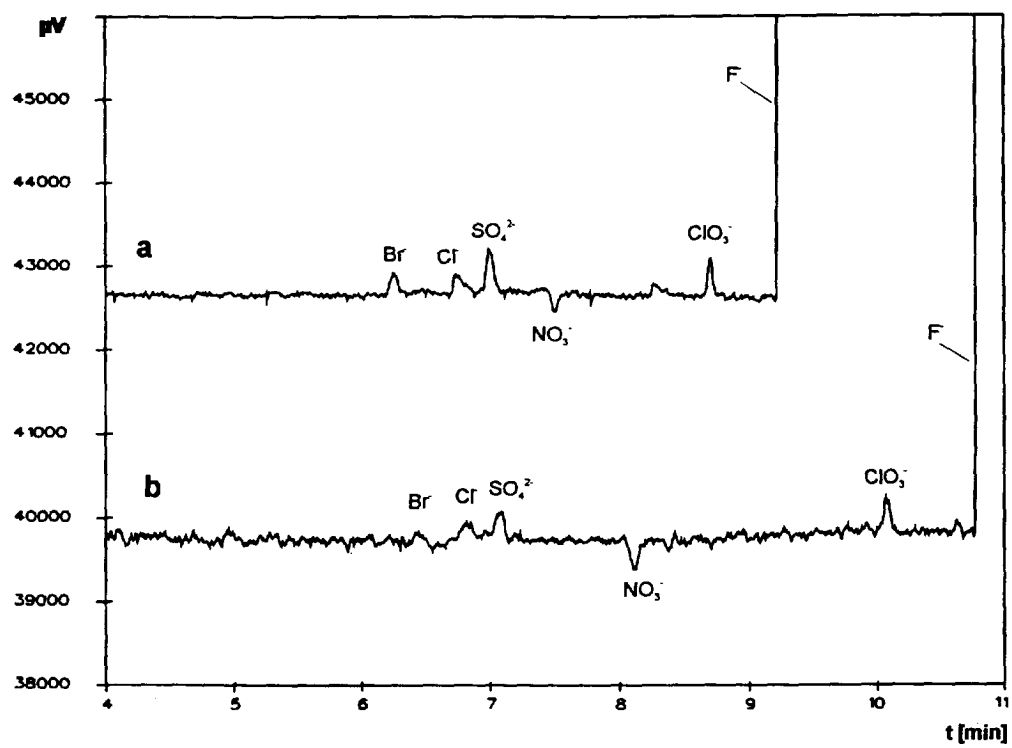

Fig. 2. Influence of the capillary I.D. (a) 50 μm I.D.; (b) 75 μm I.D. Electrolyte, 5 mM sodium molybdate; analytes, each 25 μM, HF 420 mM; capillary, fused silica, 70 cm to the detector, 86 cm total length; detection and injection, as in Fig. 1; EOF, in opposite direction to the anions. (a) $v_{EOF} = 4.5$ cm/min, (b) $v_{EOF} = 5.3$ cm/min.

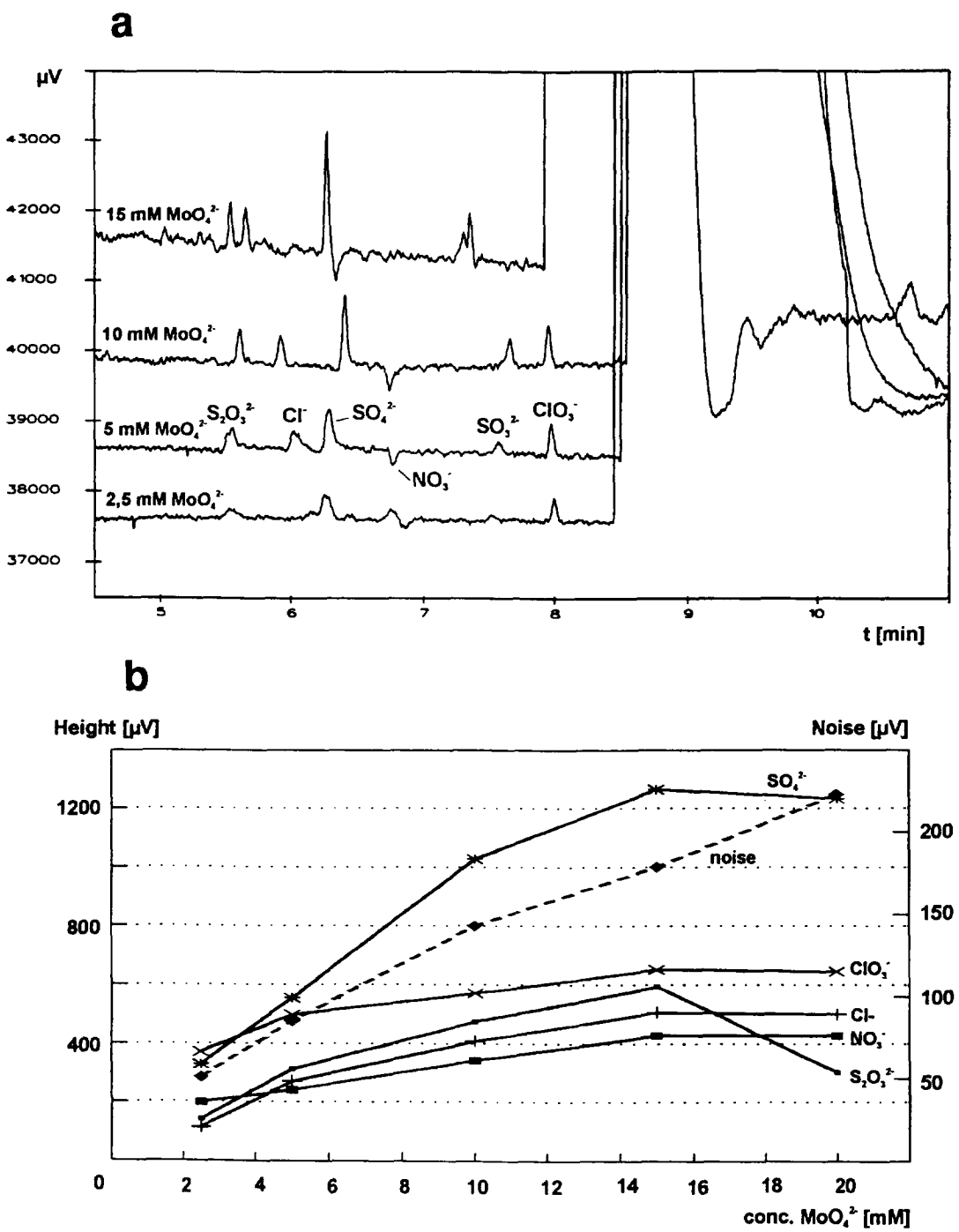

Fig. 3. Influence of the electrolyte concentration on the peak heights and on the baseline noise. (a) Electropherograms; (b) peak height and baseline noise vs. molybdate concentration. Electrolyte, different concentrations of sodium molybdate; analytes, each 25 μM, HF 420 mM; capillary, as in Fig. 2a; detection and injection, as in Fig. 1; EOF, in opposite direction to the anions, for all electrolyte concentrations nearly constant, $v_{EOF} = 3.4$ cm/min.

enlarged the peaks and increased the plate numbers. Using 10 m*M* molybdate electrolyte, the ATMR was calculated to be $1:4 \cdot 10^4$. Simultaneously, the increased baseline noise as a result of the increasing baseline signal (Fig. 3b) limited the linear response range of indirect detection. We found the optimum molybdate concentration to be within the range 8–12 m*M*. Theoretically, for direct UV detection the electrolyte concentration can be higher and is limited only by the current increase and the Joule heating.

Additionally, it can be recognized that the thiosulfate, sulfate and sulfite analyte ions migrate more slowly than the other ions when the molybdate concentration is raised. The reason is a shift in the solvation equilibrium [26,27] in the presence of an increasing counter ion (Na) concentration.

In Figs. 1–3 it was shown that by the optimization of the normal CZE run (concentration, capillary), the maximum ATMR can be increased by a factor of 4. These figures demonstrated both the capacity and the limits of CZE in the presence of a matrix ion. For many applications, an ATMR of $1:4 \cdot 10^4$ for fluoride is sufficient, but for further improvement a different approach is necessary, e.g., by using a combination of ITP and CZE.

3.2. *Determination of small inorganic anions with an ITP initial state*

During the initial stages of the separation, analyte ions can be preconcentrated in the ITP state, provided that the mobilities of the analyte ions lie between the mobilities of the electrolyte co-ion and the matrix ion. In our case, the electrolyte co-ion must have a higher mobility than the slowly migrating fluoride matrix ion and than the analyte ions to be suitable as the leading ion. On corresponding mobility data terms, chromate [28] was chosen as a leading ion (Table 1).

Because of the high pH of aqueous potassium chromate solution (7.9), the EOF is high in the direction opposite to that of the migration of the anions, thereby extending the analysis time unnecessarily. Therefore, the EOF modifier TTAOH was added to the solution to reverse the EOF. TTAOH was chosen because the common modifier TTAB produces a system peak at the migration time of bromide [22].

In contrast to the findings with molybdate as electrolyte, the peak heights of chloride, sulfate and nitrate analytes increased with increasing fluoride concentration when the chromate electrolyte was applied (Fig. 4). Having a mobility similar to that of chromate, bromide was not preconcentrated by ITP and, therefore, the peak height of bromide decreased.

From the results in Fig. 4, we estimated an improved ATMR of $1:4 \cdot 10^4$ for nitrate and of $1:6 \cdot 10^4$ for chloride and sulfate. The limit of detection (defined as twice the noise in concentration units) was found to be 3 μM for sulfate and 5 μM for chloride and nitrate (2σ) under initial ITP conditions.

Further improvement of the ATMR was limited by the worsening resolution of the analyte ions due to the increased fluoride concentration. An explanation for this effect is the prolongation of the electrodispersive depletion of the matrix ion with increased concentration of the matrix. Therefore, chromate ions need a longer time to migrate forwards through the matrix and the analyte zones, thereby starting the CZE mode. With on-line ITP–CZE coupling this leads to an increased influence of the ITP state and hence to a poorer resolution in the electropherogram. Furthermore, the analyte ions are covered one by one by the broadening of the fluoride peak. This effect can be reduced by the use of a longer capillary, but then a compromise between separation and analysis time must be found.

Under the optimized conditions, we determined the blank value of hydrofluoric acid, and so a chloride signal was detected. To determine the expected chloride contamination, the standard additions method was applied using the conditions given in Fig. 4. The regression coefficient of the calibration line of the peak area of chloride was calculated to be $r = 0.998$. Thus, we found 15 μM of chloride in 560 m*M* of hydrofluoric acid, i.e., 0.6 m*M* in the hydrofluoric acid (40%).

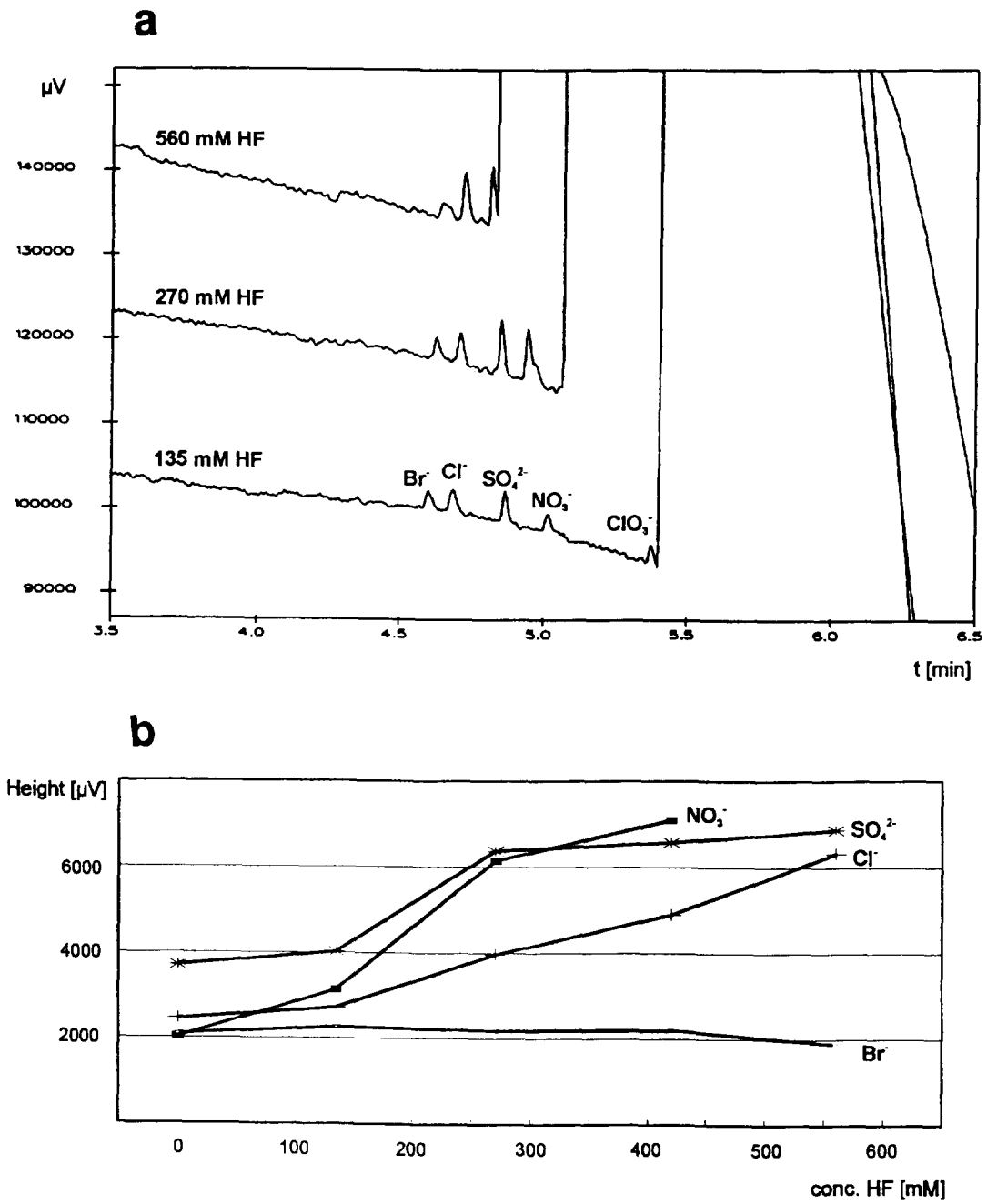

Fig. 4. Influence of HF on the peak heights using chromate as electrolyte. (a) Electropherograms; (b) peak height vs. concentration of HF. Electrolyte, 7.5 m*M* potassium chromate–0.2 m*M* TTAOH (pH 8.5); analytes, each 25 μM; capillary, 70 cm to the detector, 86 cm total length, 50 μm I.D.; detection, indirect UV at 254 nm; injection, hydrostatic (10 cm, 30 s); EOF, in the same direction as the anions, $v_{EOF} = 1.1$ cm/min.

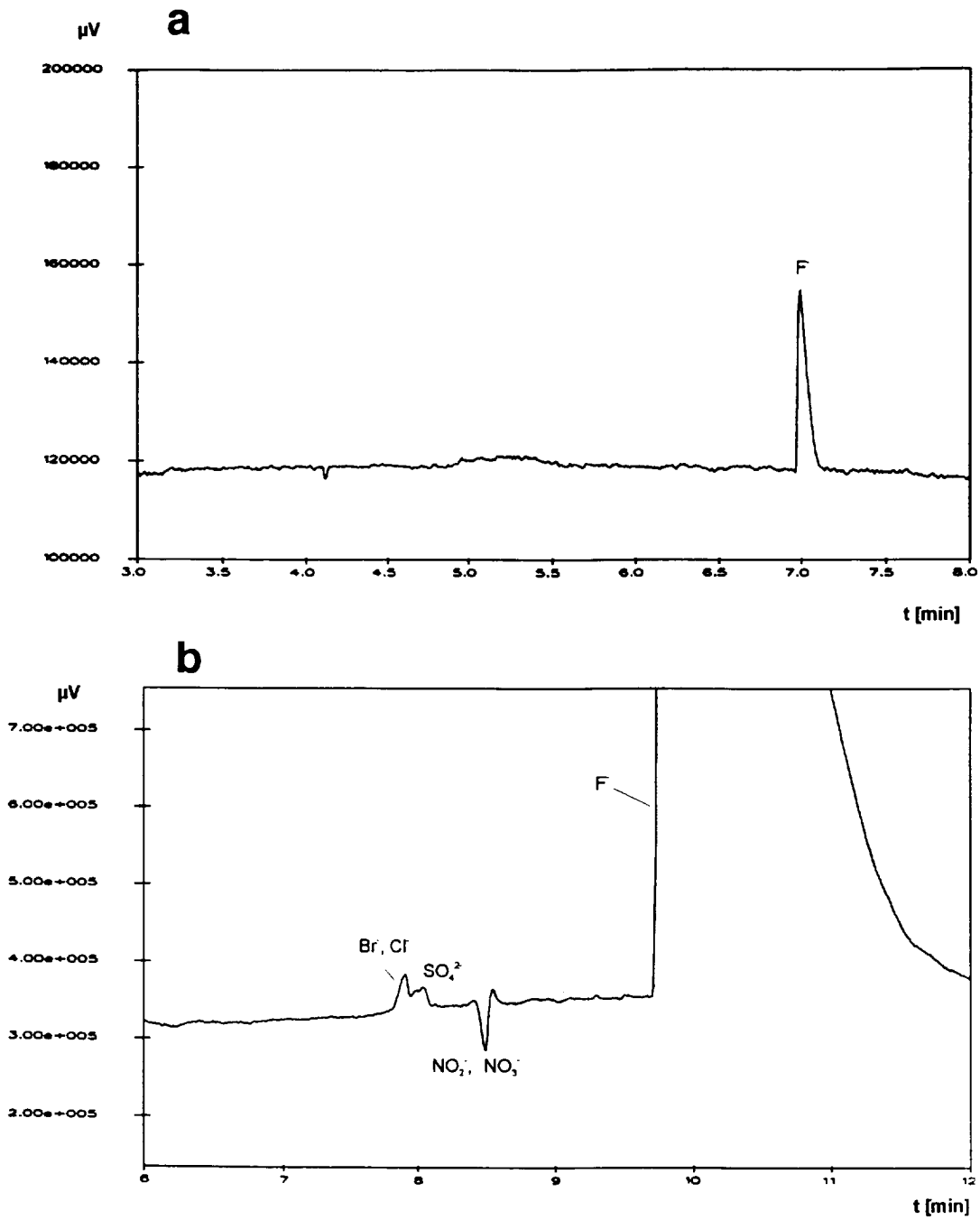

Fig. 5. Determination of anionic impurities on a silicon wafer (a) Hydrostatic injection (conditions as in Fig. 1); sample, 100-μl water droplet from repeated scanning of the wafer surface. (b) Sample stacking using molybdate electrolyte. Electrolyte, 7 m*M* sodium molybdate (pH 6.7); sample, as in (a); Injection (to prevent contamination of the sample droplet, the capillary was dipped into deionized water before it was transferred into the sample vial), hydrodynamic up to the detector (2.6 μl); all other conditions as in Fig. 1. (c) Sample stacking using chromate electrolyte. Electrolyte, 6 m*M* potassium chromate – 0.07 m*M* TTAOH (pH 8.1); capillary, as in Fig. 1; detection, as in Fig. 4; sample, as in (a); injection, as in (b); EOF, in opposite direction to the anions, $v_{EOF} = 2.1$ cm/min.

3.3. Analysis of low anionic contamination on as-polished silicon wafers

Only fluoride was detected under the hydrostatic CZE conditions (Fig. 5a) with a water droplet sample obtained by the applied microdissolution technique [19–21]. In order to decrease the detection limit, the sample had to be enriched by electrokinetic injection or by sample stacking [29]. We preferred sample stacking because analyte discrimination does not take place and peak correction is not necessary. The sample stacking was performed by filling the capillary with the sample up to the detector, resulting in a sample volume of 2.6 μl. After applying a high voltage, the analyte ions migrate rapidly towards the boundary between the sample and electrolyte. Simultaneously, the reverse-directed EOF removes the stacked cations and the water plug from the capillary. When the water plug leaves the capillary, a uniform field strength is reached and the CZE separation begins by itself. The sample stacking results are shown in Fig. 5b. Applying molybdate electrolyte it was possible to detect the presence of chloride, sulfate and nitrate ions. As can be seen, fluoride is enriched by sample stacking and acts as a matrix ion. However, owing to the described matrix effects, the detected species could not be quantified using the molybdate electrolyte.

To improve the separation, we adjusted the conditions of initial ITP also for sample stacking. Using chromate electrolyte with small amounts of the organic modifier TTAOH, the EOF was not reversed but slowed (Fig. 5c). Under these optimized conditions, bromide, chloride, sulfate, nitrite, oxalate and nitrate were detected. The peak identification was carried out using the standard additions method. Oxalate was identified on wafer surfaces for the first time. The reason for this contamination must be investigated.

For quantification of the analytes, the influence of the matrix ion on the peak shape, resulting in systematic errors for peak integration, must be accounted for. Therefore, the stock standard solutions for calibration (four solutions in the range 0.05–5 μM for the analytes) were applied in fluoride matrices similar to

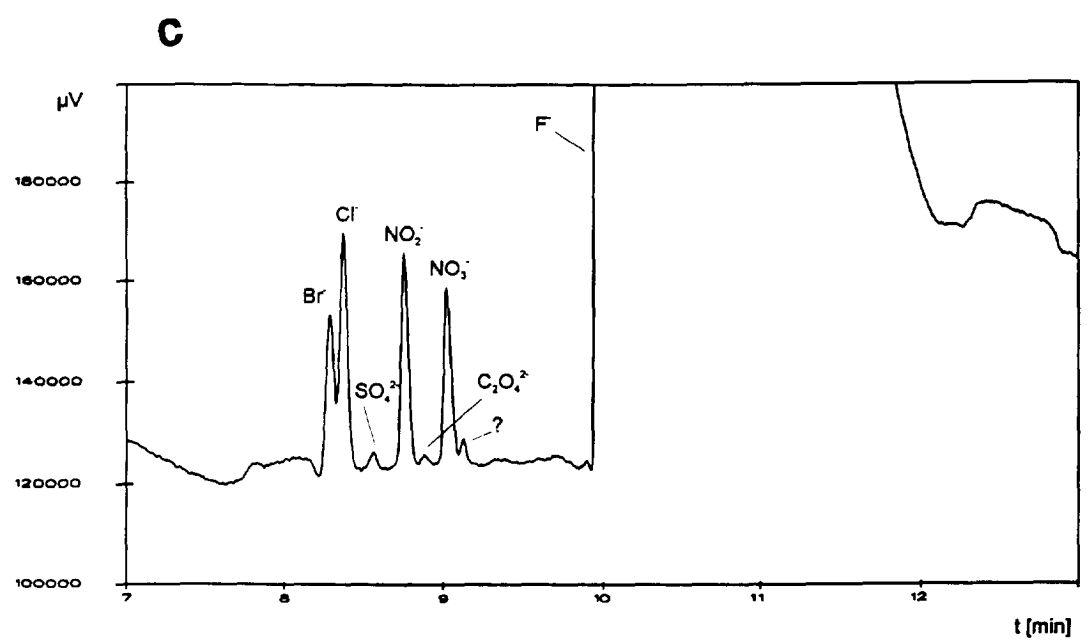

Fig. 5. (contd).

Table 2
Surface concentrations and absolute values of anionic contamination on as-polished silicon wafers after different experimental cleaning analysed with sample stacking

Sample	*Parameter*	*Anion*[a]						
		Bromide[b] ($r = 0.985$)	Chloride[b] ($r = 0.995$)	Sulfate ($r = 0.989$)	Nitrite ($r = 0.982$)	Oxalate[c] ($r = 0.983$)	Nitrate ($r = 0.989$)	Chlorate ($r = 0.993$)
Ultra-pure water blank	Concentration (μmol/l)	<0.05	0.3	0.05	0.05	<0.05	0.1	<0.05
Preclean[d] sample 1	Concentration (μmol/l)	4.4	1.6	0.35	0.6	<0.01	1.5	0.9
	Absolute value (10^{10} anions/cm^2)	151	55	12	21	<0.34	51	31
Repeated scanning	Concentration (μmol/l)	151.3	2.7	0.07	2.7	0.07	1.9	<0.02
	Absolute value (10^{10} anions/cm^2)	45	92	2.4	92	2.4	65	<0.69
Preclean[d] sample 2	Concentration (μmol/l)	3.4	0.7	0.3	0.5	<0.01	0.8	1.0
	Absolute value (10^{10} anions/cm^2)	116	24	10	17	<0.34	27	34
Repeated scanning	Concentration (μmol/l)	2.4	1.2	0.02	0.7	0.14	14	0.2
	Absolute value (10^{10} anions/cm^2)	82	41	0.68	24	4.8	48	<0.69
Clean A[d]	Concentration (μmol/l)	3.8	2.6	0.15	3.5	0.10	2.3	<0.2
	Absolute value (10^{10} anions/cm^2)	130	89	5.1	120	3.4	79	<0.69
Clean B[d]	Concentration (μmol/l)	1.5	1.5	0.04	1.15	0.09	2.1	<0.2
	Absolute value (10^{10} anions/cm^2)	51	51	17	39	3.1	72	<0.69

[a] r = Regression coefficient.
[b] Bromine and chlorine form surface species with pure silicon which are apt to hydrolyse.
[c] In the given analytical environment, low-molecular-mass acids such as oxalic acid can also be formed on the pure silicon wafer.
[d] Cleaning technology based on RCA cleaning that involves wet alkaline and acid oxidation to silicon [30].

the solved samples. The calculated regression coefficient are given in Table 2. It can be seen that the quality of the calibration lines was only moderate. The reason for this could be variations of the injection volume and of the EOF. The data show impurity concentrations in the range of $3 \cdot 10^{10}$ oxalate anions/cm^2 to $1.3 \cdot 10^{12}$ bromide ion/cm^2 (Table 2).

For recovery studies, bromide and sulfate were selected. Bromine (and more vigorously chlorine) can react with silicon and forms compounds that are unstable in hydrolysis with aqueous hydrofluoric acid solution. Sulfate does not react with silicon and therefore can be used as a standard ion for clean room conditions, since its concentration cannot be changed by chemical reaction. We obtained lower recoveries for bromide (70–30%) than for sulfate (80–93%).

4. Conclusions

We determined the optimized conditions of CZE to determine anionic analytes in samples preconcentrated on as-polished silicon wafer surfaces with an excess of fluoride solution. The combination of an electrophoretic separation with the initial ITP state was a very effective approach in improving the power of detection in the presence of matrix ions without modifying the basic CZE system. Our results suggest that an appropriate selection of the electrolyte co-ion diminishes the limitations due to the matrix ion, and that a detection power of $1:6 \cdot 10^4$ ATMR can be achieved. This ATMR value represents a six-fold increase over the results obtained in the normal CZE mode. Hence, the presence of matrix ions with a mobility very different from the mobilities of the analytes can be of advantage. In this work, the increase in plate numbers resulted in an additional improvement in the detection limits by a factor of two.

The optimization of the CZE conditions is more complicated when the mobility of the matrix ion is similar to the mobilities of the analytes. On the one hand, the analyte peaks can co-migrate with the matrix peak even at low matrix ion concentrations. On the other hand, taking the simultaneous impact of the co-ion on the ITP conditions into account, the selected co-ion must be a subtle compromise between measurement of analytes with higher or with lower mobilities than the matrix ion.

Even during calibration by sample stacking, initial ITP conditions must prevail. The quantification was carried out using calibration standard solutions with fluoride concentrations similar to those in the sample. In this way, we achieved a power of detection sufficient for surface analyses down to $5 \cdot 10^9$ ions cm^{-2}.

The mobile organic anion oxalate was identified on as-polished, experimental silicon wafer surfaces for the first time. In the same manner, electronic-grade hydrofluoric acid can be analysed for traces of anionic contaminants.

References

[1] L. Fabry, L. Köster, S. Pahlke, L. Kotz and J. Hage, *Proc. Electrochem. Soc.*, 15 (1993) 193, *and references cited therein.*
[2] L. Fabry, S. Pahlke, L. Kotz and G. Tölg, *Fresenius' J. Anal. Chem.*, 349 (1994) 260.
[3] L. Fabry, S. Pahlke, L. Kotz, E. Schemmel and W. Berneike, *Proc. Electrochem. Soc.*, 15 (1993) 232.
[4] M. Platt and J. Leo, *J. Chromatogr.*, 546 (1991) 347.
[5] D. Rathmann, *Proc. Electrochem. Soc.*, 12 (1992) 816.
[6] D. Rathmann and L. Fabry, *Proc. Electrochem. Soc.*, 12 (1992) 344.
[7] T. Talasek, B. Lucero and L. Vanatta, *Microcontamination*, 27, No. 9 (1994) 56.
[8] P. Kim Gupta, S.H. Tan, Z. Pourmotamed, F. Cristobal, N. Oshiro and B. McDonald, in *Proceedings of Electrochemical Society Spring Meeting, May 1994, San Francisco*, in press.
[9] D.S. Stegehuis, H. Irth, U.R. Tjaden and J. van der Greef, *J. Chromatogr.*, 538 (1991) 393.
[10] D.S. Stegehuis, U.R. Tjaden and J. van der Greef, *J. Chromatogr.*, 591 (1992) 341.
[11] F. Foret, V. Sustacek and P. Boček, *J. Microcol. Sep.*, 2 (1990) 229.
[12] N.J. Reinhoud, U.R. Tjaden and J. van der Greef, *J. Chromatogr. A*, 653 (1993) 303.
[13] D. Kaniansky and J. Marak, *J. Chromatogr.*, 498 (1990) 191.
[14] F. Foret, E. Szoko and B.L. Karger, *J. Chromatogr.*, 608 (1992) 3.

[15] J.L. Beckers and F.M. Everaerts, *J. Chromatogr.*, 508 (1990) 3.
[16] J.L. Beckers and F.M. Everaerts, *J. Chromatogr.*, 508 (1990) 19.
[17] V. Dolnik, K.A. Cobb and M. Novotny, *J. Microcol. Sep.*, 2 (1990) 127.
[18] P. Gebauer, W. Thormann and P. Boček, *J. Chromatogr.*, 608 (1992) 47.
[19] A. Huber, H. Rath, P. Eichinger, T. Bauer, L. Kotz and R. Staudigl, *Proc. Electrochem Soc.*, 20 (1988) 109.
[20] T. Shiraiwa, N. Fujino, S. Sumita and Y. Tanizoe, *ASTM Special Technical Publication*, No. STP 850, ASTM, Philadelphia, 1988, p. 314.
[21] A. Shimazaki, H. Hiratsuka, Y. Matsushita and S. Yoshii, in *Extended Abstracts 16th Conference on Solid State Devices and Materials, Kobe, 1984*, p. 281.
[22] A. Röder and K. Bächmann, *J. Chromatogr. A*, 689 (1995) 305.
[23] S. Hjertén, *Electrophoresis*, 11 (1990) 665.
[24] *CRC Handbook of Chemistry and Physics*, CRC Press, Boca Raton, FL, 71st ed., 1991.
[25] S. Hjertén and M. Kiessling-Johansson, *J. Chromatogr.*, 550 (1991) 811.
[26] T. Groh and K. Bächmann, Electrophoresis, 13 (1992) 458.
[27] K. Bächmann, J. Boden and I. Haumann, *J. Chromatogr.*, 626 (1992), 259.
[28] W.R. Jones and P. Jandik, *Am. Lab.*, 22 (1990) 51.
[29] R.L. Chien and D.S. Burgi, *Anal. Chem.*, 64 (1992) 1046.
[30] W. Kern and D.A. Puotinen, *RCA Rev.*, 31 (1970) 187.